

## Phase Transitions, Domains Walls and Defects Dynamics of LaAlO<sub>3</sub> via *In Situ* Heating in the Transmission Electron Microscope

Qingyun Mao<sup>1</sup>, Megan Holtz<sup>1</sup>, Darrell G. Schlom<sup>2</sup> and David A. Muller<sup>1</sup>

<sup>1</sup>. School of Applied and Engineering Physics, Cornell University, Ithaca, New York 14853, USA

<sup>2</sup>. Department of Materials Science and Engineering, Cornell University, Ithaca, New York 14853, USA

Many materials processes are thermally activated, and a full understanding of the microscopic details often requires characterization on the nanoscale. *In situ* heating in the TEM is a powerful technique for observing temperature effects on the atomic scale. We use *in situ* TEM to study octahedral rotations, which play a key role in the strain-driven coupling of order parameters in multifunctional transition metal oxides. In LaAlO<sub>3</sub> (LAO), these rotations drive a continuous improper ferroelastic phase transition from a rhombohedral (*R-3c*) to cubic (*Pm-3m*) perovskite structure ( $T_c \sim 540^\circ\text{C}$ ). This phase change is the result of distortions of the oxygen-sublattice, without changing the periodicity of the cation sublattice. Here we perform *in situ* heating of bulk LAO single crystals. We observe the phase transition with diffraction, and also observe twin-boundaries and defect motion by STEM at high temperatures.

*In situ* heating of LAO was performed on a 200 kV FEI Tecnai F20, with the new Protochips Aduro chip-based double-tilt heating holder. The specimen was prepared by FIB from a single crystal, along the (011) direction to observe octahedral rotations. The LAO was heated from room temperature (RT) to above  $T_c$ . Diffraction patterns were recorded as a function of temperature to probe the phase of the LAO.

Figure 1(a) shows the decreasing intensity of the rhombohedral diffraction spots relative to the primary cubic diffraction spots as the sample was heated to  $T_c$ . Surprisingly, above  $T_c$ , the diffraction spots associated with the rhombohedral structure did not completely disappear, although they were faint (Figure 1(c)), which deviates from previous results using neutron diffraction [1]. This may be due to a rhombohedral phase pinned at the surface, even above the bulk transition temperature.

LAO has micro-twinned domains, and the domain wall width increases with increasing temperature, diverging at  $T_c$  [2]. To image the walls, we use low-angle annular dark field (LAADF) and bright field (BF) images taken simultaneously (Figure 2). LAADF images help locate the heavy cations and show uniform contrast. BF images, which are more sensitive to the oxygen-sublattice, show domains with a longer periodicity in the middle-left region. A diffractogram of the middle region and bottom-right corner indicates that it is likely there is a grain boundary between regions with (010)<sub>pc</sub> and (001)<sub>pc</sub> twins, viewed along zone axis [011]<sub>pc</sub>, as the superlattice reflections only show up along zone axis [011]<sub>pc</sub>, not along [01-1]<sub>pc</sub>. Upon cooling, we saw the formation of a grain boundary, which upon heating disappeared, a result previously inferred from indirect x-ray diffraction measurements [2].

Previous studies reported an increase in conductivity in LAO at about 400°C [1], interpreted as static vacancies becoming dynamically disordered. Our single crystal LAO, as is typical for Czochralski growth, is Al-rich [3]. We expect the nonstoichiometry to be accommodated by defects such as La-O vacancy clusters. To study defect dynamics, we heated a specimen up to 1000°C. High densities of point defect clusters are shown in LAADF and BF images (Figure 3). The contrast of the defects (dark in HAADF, bright in LAADF) suggests that they arise from strain fields [4]. The defects were not visible at high temperatures, but

reappeared after cooling to RT. Comparing the positions of the defects before and after annealing, many of the clusters reappeared in the same positions, although smaller in size [5].

#### References:

- [1] S. A. Hayward *et al*, Physical Review B **72**, 054110 (2005). [2] J. Chrosch and Ekhard K. H. Salje, J. Appl. Phys. **85**, 722 (1999). [3] G. W. Berkstresser *et al*, Journal of Crystal Growth **128**, 684 (1993). [4] Z. Yu *et al*, J. Appl. Phys. **95**, 3362 (2004).  
 [5] Work supported by DOE Basic Energy Sciences SISGR award #DE-SC0002334. Facilities support from the Cornell Center for Materials Research, an NSF MRSEC (DMR-1120296).

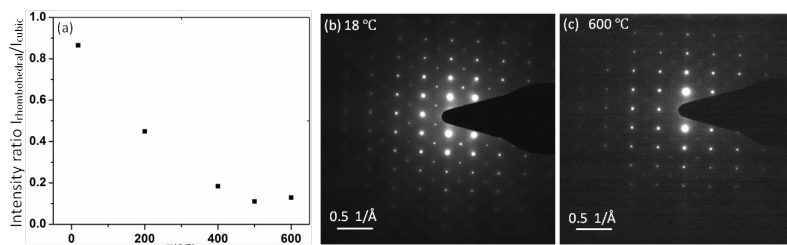


**Figure 1.** (a) The intensity of the diffraction spots from rhombohedral structure (such as 2,-3,5 in hexagonal coordinates) relative to that of diffraction spots from cubic structure (such as 3,1,-1 in cubic lattice). The intensity amplitude is obtained by Gaussian fitting of each spot. Zone axis [011]pc. (b) Diffraction pattern taken at room temperature before heating. (c) Diffraction pattern taken at 600 °C.

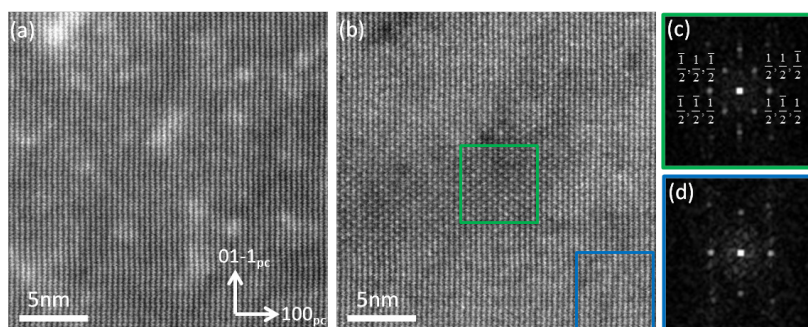


**Figure 2.** (a) LAADF and (b) BF images taken simultaneously after cooling. Zone axis [011]pc. (c) and (d) are diffractograms of the corresponding regions in the colored squares. The four labeled diffraction spots are kinematically forbidden, but useful fingerprint of the rhombohedral structure.

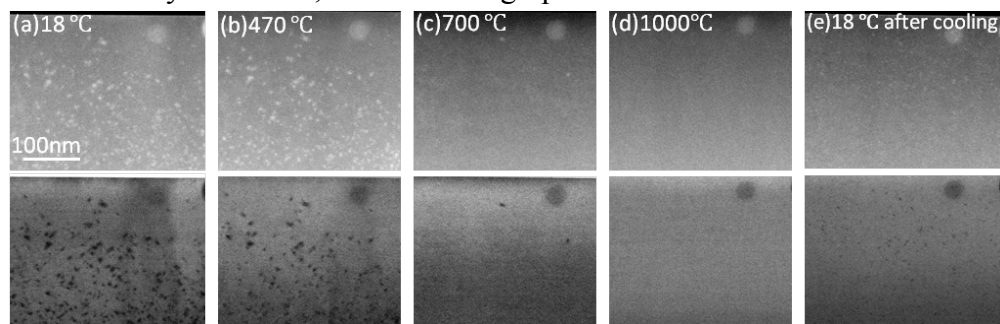


**Figure 3.** LAADF and BF images taken simultaneously during a heating and cooling cycle. The top row are LAADF images and the bottom row are BF images. (a) 18 C; (b) 470C; (c) 700C; (d) 1000C; (e) 18C after cooling.